RSC Advances

ROYAL SOCIETY OF CHEMISTRY

www.rsc.org/advances

Journal Name

ARTICLE

Synthesis and characterization of nanostructured PS-*b*-P4VP/Fe_2O_3 thin films with magnetic properties prepared by solvent vapor annealing

Received 00th January 20xx,
Accepted 00th January 20xx

DOI: 10.1039/x0xx00000x

www.rsc.org/

I. Barandiaran[a] and G. Kortaberria[a]

In this work hybrid organic/inorganic nanocomposites with magnetic properties, based on PS-*b*-P4VP block copolymer and Fe_2O_3 maghemite nanoparticles have been prepared. Nanoparticles were surface modified with PS brushes by *grafting through* method. The morphology of neat block copolymer and nanocomposites was analyzed by AFM. For nanostructuring, thin films were annealed under dioxane vapors, a selective solvent for the PS block. Morphology of neat copolymer thin films changed from hexagonal to stripped with exposure time. The addition of the nanoparticles also modified the morphology of the nanocomposites, especially the higher nanoparticle contents. For all cases nanoparticles were selectively dispersed into PS domains. Moreover, magnetic characterization by VSM and SQUID has demonstrated that magnetic properties of nanoparticles have been transferred to the nanocomposites.

Introduction

Organic/inorganic nanocomposites constitute an important sort of new age material that attracted an important amount of research[1-3]. Engineering the self-assembly of inorganic nanoparticles within block copolymer nanodomains is useful for the design of periodic structures, obtaining materials with enhanced mechanical strength as well as unique optical, electronic and magnetic properties at the nanometer scale[4-8], for various fields of application such as photonic, band gap materials, solar cells, sensors, and high-density magnetic storage devices[1, 9-11], among others. Several works have been carried out about nanocomposites based on block copolymer and magnetic nanoparticles[7, 8, 12-14], in order to prepare hybrid films with magnetic properties interesting for applications as high density magnetic storage media, thermoresponsive magnetic sensors, drug carriers or targeted drug release. Due to the ability of block copolymers to self-assembly into various periodic structures depending on the nature of the blocks, molecular weight and composition, and processing characteristics, they constitute a versatile platform material for embedding inorganic nanoparticles[4-16].

When preparing nanocomposites based on block copolymer and inorganic nanoparticles two main challenges should be overcame: how to obtain the desired nanostructure for the block copolymer matrix in the presence of nanoparticles, and the proper dispersion of the nanoparticles. For nanostructuring the block copolymer different parameters such as copolymer composition, Flory-Huggins interaction parameter among both blocks and polymerization degree of the copolymer[17, 18] should be taken into consideration. During the last years different techniques have been used for nanostructuring block copolymer thin films: thermal annealing[19], control of interfacial interaction[20], solvent vapor annealing (SVA)[21], electric field[22, 23], chemical pre-patterning[24], graphoepitaxy[25] or epitaxial growth[26]. When nanostructuring of thin films is carried out by SVA, solvent election is of crucial importance, as the solvent can determine the obtained morphology[21]. The solubility of a non-polar polymer in a solvent is determined by the Flory-Huggins interaction parameter (equation 1), which can be obtained from the solubility parameter (equation 2) of the components. A polymer is considered to be soluble in a solvent if $\chi \leq 0.5$[27].

$$\chi \approx 0{,}34 + \frac{V}{RT}(\delta_P - \delta_S)^2 \quad (1)$$

$$\delta = \sqrt{\frac{E_{coh}}{V}} = \sqrt{\frac{\Delta H_V - RT}{V}} \quad (2)$$

Where χ is the Flory-Huggins interaction parameter, V solvent specific volume, R ideal gas constant, T temperature, δ solubility parameter, E_{coh} cohesive energy and ΔH_V enthalpy of vaporization.

On the other hand, to overcome the problem of nanoparticle tendency to aggregate due to their high surface area and surface energy, and to facilitate their selective dispersion in one of the blocks of a block copolymer, different routes have been used. One of them has been the use of surfactants. In that way, Emrick et al.[28] controlled the surface hydrophobicity by using different surfactants in order to disperse CdSe

[a] "Materials + Tecnhologies" Group, Euskal Herriko Unibertsitatea (UPV/EHU) Plaza de Europa 1, 20018 Donostia, Spain.
DOI: 10.1039/x0xx00000x

nanoparticles in poly(styrene-*b*-2-vinylpiridine) (PS-*b*-P2VP) copolymer, creating hierarchically ordered patterns with CdSe nanoparticles located in PS or P2VP domains depending on the surfactant. The electrophoretic deposition of nanoparticles has been other of the used methods. In this way, Zhang et al.[29] placed CdSe nanoparticles in diblock copolymer templates. Also the so-called *in situ* approach (nanoparticles are directly synthesized within a block copolymer domain from metal precursors) has been used for incorporating inorganic nanoparticles into block copolymer nanostructures. Cohen et al.[30] prepared nanocomposites based on poly(styrene-*b*-acrylic acid) (PS-*b*-PAA) copolymer and metallic nanoparticles of Pd, Cu, Au and Ag following this method.

Another common method for achieving the placement of nanoparticles into desired nanodomains is the growth of polymer brushes on the surface of nanoparticles. There are essentially three techniques to chemically graft polymers on nanoparticles surface: *grafting to*[31, 32], *grafting from*[33, 34] and *grafting through*[35-37]. In the first method (*grafting to*) an end-functionalized polymer reacts with the reactive sites on nanoparticle surface. In the *grafting from* method the polymer chains grow in situ from an initiator that has been previously anchored to nanoparticle surface. In the *grafting through* technique, molecules attached to the surface present a group suitable for polymerization (usually a silane with terminal vinyl groups). Nanoparticles present in the polymerization medium are covered by the polymer. Obtained grafting densities are usually higher than those obtained by *grafting to* being the technique easier to carry out than *grafting from* one, even if obtained grafting densities used to be lower[38]. *Grafting through* has been demonstrated to be a relatively easy technique to modify nanoparticles for placing at desired nanodomains[37, 39].

In this work maghemite nanoparticles were modified by *grafting through* method. PS polymer brushes were successfully grown through the surface of the nanoparticles. The functionalization of nanoparticles increasing their compatibility with one of the blocks provides the way to prepare hybrid nanocomposites based on maghemite nanoparticles selectively placed at PS domains of PS-*b*-P4VP block copolymer nanostructured by SVA. Morphology evolution with annealing time and nanoparticle content was analyzed by atomic force microscopy (AFM). Magnetic characterization of the nanocomposites was also carried out, finding that nanoparticles transferred their magnetic properties to the nanocomposite after modification and dispersion into block copolymer.

Experimental

Materials

Maghemite (Fe_2O_3) nanoparticles with a nominal size of 9 nm were purchased from Integram Technologies, Inc. 3-methacryloxypropyltrimethoxysilane (MPTS), with 98% of purity, was purchased from ABCR. The initiator 2,2'-azobisisobutyronitrile (AIBN), used without further purification, and styrene monomer, with a purity of 99 %, distilled under reduced pressure over CaH_2 before use, was purchased from Aldrich. Poly(styrene-*b*-4-vinylpyridine) (PS-*b*-P4VP) block copolymer was purchased from Polymer Source with number average molecular weight (Mn) of 22,500 and 29,000 g/mol for polystyrene (PS) and poly(4-vinyl pyridine) (P4VP) blocks, respectively, and a polydispersity index (Mw/Mn) of 1.2 for both blocks.

Nanoparticle modification

Silanization process. Fe_2O_3 nanoparticles were first modified with MPTS. This reaction implies a nucleophilic attack of –OH groups at nanoparticle surface to the Si atoms of MPTS. 0.05 g of nanopaticles and 10 µmol of silane were mixed by sonication into 40 mL of toluene. The reaction was carried out at inert atmosphere for 3 h at 60 °C. Nanoparticles were subsequently washed with THF, until any silane rest was eliminated (the presence of silane after washing was probed by FTIR), and dried in vacuum for 72 h at 40 °C.

***Grafting through* process.** Once the maghemite nanoparticles were silanized, their surface modification with PS brushes by *grafting through* method was carried out. 0.02 g of silanized Fe_2O_3 nanoparticles and 0.1 g of AIBN were dispersed into 40 mL of toluene and then 2 mL of monomer were added. The reaction was carried out at inert N_2 atmosphere at 70 °C for 5 h. Modified nanoparticles were subsequently washed with THF, until any monomer rest was eliminated (probed by FTIR), and dried in vacuum for 72 h at 40 °C.

Nanocomposite preparation

Nanocomposites were prepared mixing PS-*b*-P4VP block copolymer with functionalized Fe_2O_3 nanoparticles. Nanoparticles were first dispersed in toluene for 2 h by sonication, and PS-*b*-P4VP block copolymer was added. Thin films were then prepared by spin-coating onto Si(100) wafers at 2000 rpm for 120 s using a Telstar Instrumat P-6708D spin-coater. For selective solvent annealing, thin films were exposed to saturated dioxane vapors for different period of exposure into a closed vessel and kept at room temperature after spin-coating, without removing the residual solvent. After exposure samples were removed and stored at room atmosphere before characterization. Nanocomposites were prepared from 1 to 5 wt% of nanoparticles.

Characterization techniques

Fourier transformed infrared spectroscopy (FTIR) was carried out with a Nicolet Nexus 600 FTIR spectrometer, performing 20 scans with a resolution of 4 cm^{-1}.

Thermogravimetric analysis (TGA) was performed with a Mettler Toledo TGA/SDTA851 instrument. Tests were carried out from room temperature to 750 °C with a heating rate of 10 °C/min.

Surface morphologies obtained for different films were studied by atomic force microscopy with a scanning probe microscopy AFM Dimension ICON of Bruker, operating in tapping mode (TM–AFM). An integrated silicon tip/cantilever, from the same manufacturer, having a resonance frequency of around 300 kHz, was used. Measurements were performed at a scan rate of 1 Hz/s, with 512 scan lines.

Magnetic measurements were performed with superconducting quantum interference device (SQUID) and vibrating sample magnetometer (VSM). The SQUID magnetometer (MPMS-7T, Quantum Design) has a superconducting magnet of 7 T, it was used to obtain the ZFC and FC curves. The VSM (CFMS, Cryogenic Ltd) has a superconducting magnet of 14 T.

Results and discussion

Nanoparticle functionalization

Before the polymerization of PS brushes nanoparticles were surface-modified with MPTS silane. The right attachment of the silane to the nanoparticle surface is of vital importance, as the addition of MPTS gives vinyl group-terminated maghemite nanoparticles. The vinyl groups in the nanoparticle surface work as the initiator for the polymerization reaction of PS brushes[35]. The success of silanization process was probed by FTIR and TGA measurements, as it can be seen in Figure 1. From FTIR spectra, the appearance of bands related with the main bonds of MPTS can be seen: C=O stretching vibration at 1704 cm^{-1}, C-O-C stretching deformation vibration at 1329 and 1300 cm^{-1}, and Si-O-Fe stretching vibration at 1176 and 1011 cm^{-1}, indicating the presence of MPTS attached to the surface. After silanization, nanoparticles were modified with PS brushes by *grafting through* method. The presence of brushes into the surface was also probed by FTIR. In the FTIR spectra (Fig 1A) of PS-modified iron oxide nanoparticles, main bands of PS such as C-H aromatic stretching vibration (3023 cm^{-1}, inner part of the figure), C-C stretching frequency of the ring in plane (1600 cm^{-1}), C-C stretching vibration of the ring in plane (1494 cm^{-1}) and C-H out of plane bending vibration of the ring (700 cm^{-1}), can be seen[40, 41], thus probing the presence of PS.

Figure 1B shows TGA thermograms of pristine, silanized and PS-modified nanoparticles. TGA measurements, besides showing the modification of the nanoparticles with the organic compound, were used to determine the amount of grafted organic part. The weight loss of unmodified nanoparticles is related to physisorbed water (until 120 °C) and surface -OH degradation (above 120 °C)[42]. For silanized nanoparticles, a significant weight loss starts at around 300 °C, which corresponds to the combustion of the silane molecules adsorbed on the surface and also to the elimination of hydroxyl groups[43]. The thermal degradation of the PS starts around 300 °C[40]. A surface density of 2.8 molecules/nm^2 has been calculated for the silane following the method used by Bartholome et al.[44]. A direct comparison of the surface density of hydroxyl groups (8.1 molecules/nm^2) and that of the silane on the surface yielded a reaction efficiency of 34.5 %. Moreover, the weight loss related to the degradation of PS can be clearly seen, thus probing the presence of the polymer in the sample.

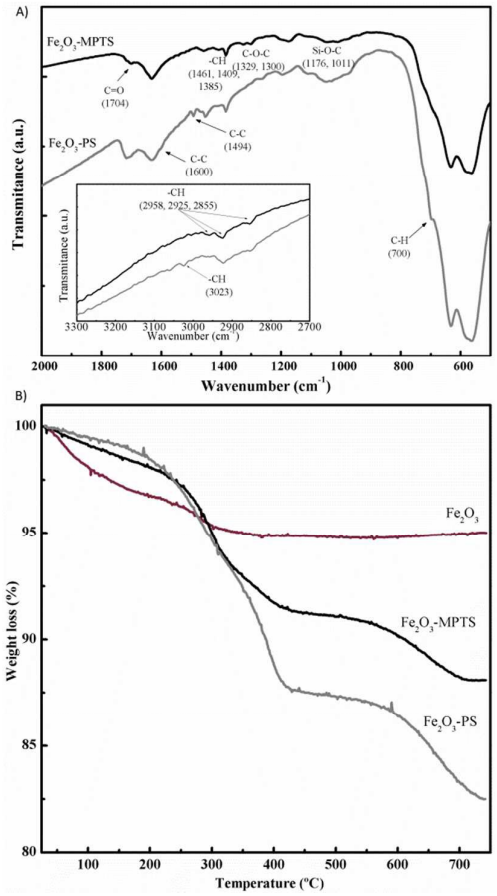

Figure 1. A) Infrared spectra of the MPTS silanized and PS polymer brush anchored nanoparticles, B) TGA thermogram of neat and silanized and PS modified Fe_2O_3 nanoparticles

Nanocomposite thin film morphology analysis

PS-*b*-P4VP block copolymer thin films, as well as those of nanocomposites were exposed to dioxane vapors, which is a selective solvent for PS block (χ_{PS}= 0.35 and χ_{P4VP}= 2.61), before being analyzed by AFM. In AFM images PS domains appear brighter than the P4VP ones[43]. When nanocomposites were prepared by spin coating without any annealing treatment (Figure 2), although soft microphase separation is observed, no ordered microstructure is formed. When films were exposed to dioxane for 24 hours (Figure 3) neat block copolymer presents a hexagonal morphology, although some stripes can be appreciated, giving a clue about the evolution that will have the morphology with longer exposure times; with the addition of 1 wt% nanoparticles the hexagonal morphology is maintained, while for higher nanoparticle amount a defined morphology is not obtained. In any case, the absence of nanoparticle agglomerations shows the good dispersion of the nanofiller.

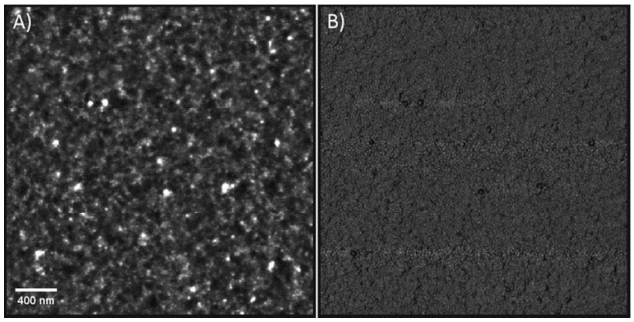

Figure 2. AFM height (A) and phase (B) images of spin coated PS-*b*-P4VP thin films

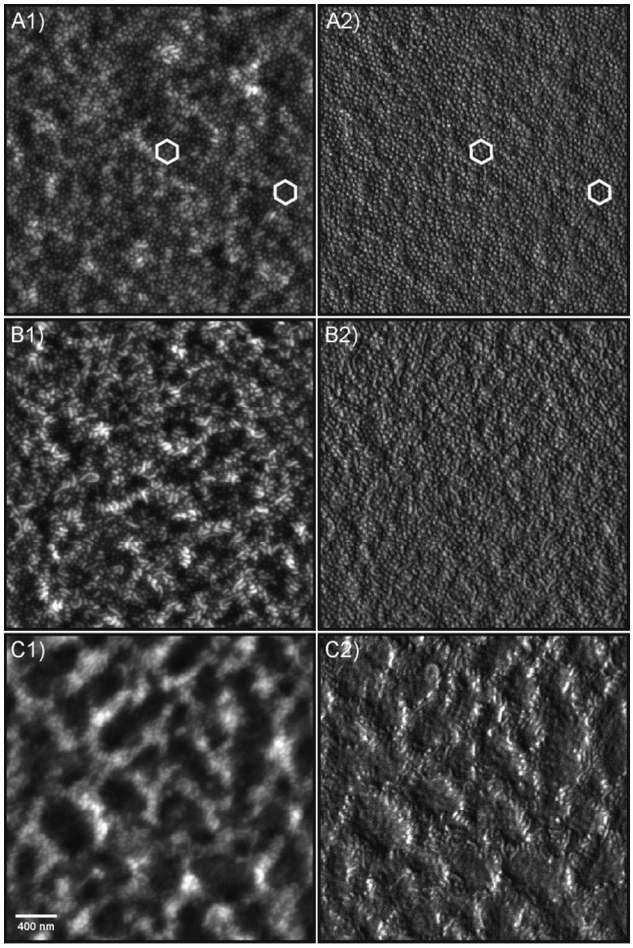

Figure 3. AFM height (1) and phase (2) images of thin films after 24 h of exposure to dioxane: A) neat block copolymer, B) nanocomposite with 1 wt% of nanoparticles and C) nanocomposite with 5 wt% of nanoparticles

For longer exposure to dioxane vapors (48 h), the morphology of the neat block copolymer evolved from hexagonal to stripped morphology (Figure 4). The neat block copolymer presents a totally stripped morphology after 48 h of exposure, with a lamellar structure normal to the substrate. When 1 wt% of functionalized nanoparticles were added the stripped morphology was maintained, despite small areas with cylinders perpendicular to the surface appeared. For higher nanoparticle amount the morphology change promoted by nanoparticles can be seen. In this way, for 5 wt% nanocomposites, few lamellas can be seen, the main morphology consisting on cylinders perpendicular to the surface. The good dispersion of nanoparticles, with the absence of remarkable agglomerations should be underlayed again.

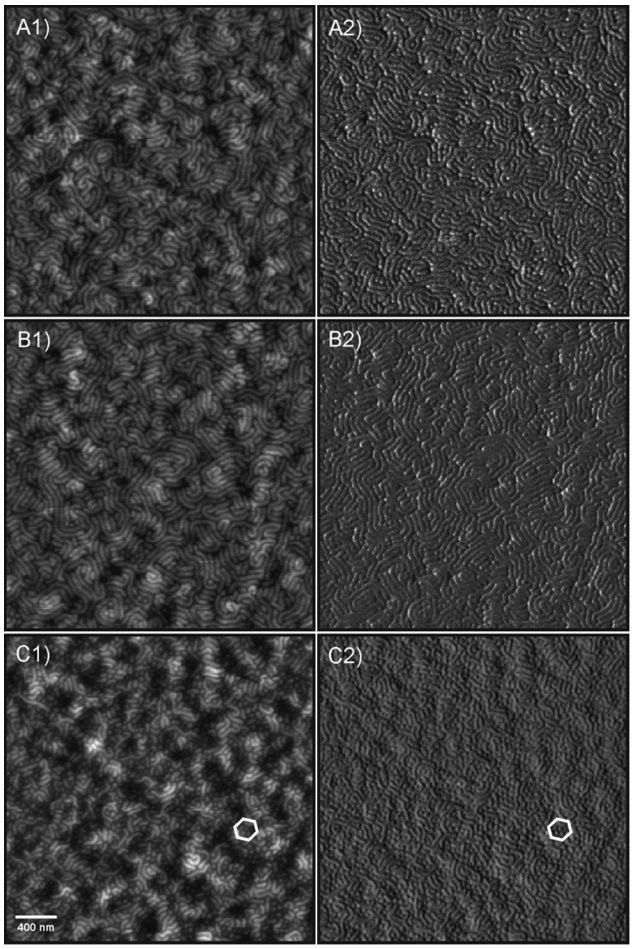

Figure 4. AFM height (1) and phase (2) images of the nanocomposites after 48 h of exposure to dioxane, A) neat block copolymer, B) nanocomposites with 1 wt% of nanoparticles and C) nanocomposites with 5 wt% of nanoparticles

The morphological evolution of the neat block copolymer with the exposure to dioxane vapors could be attributed to the migration of the PS domains to the surface[46], attracted by the dioxane molecules. When nanoparticles are added to the block copolymer at low concentration there are not remarkable effects, but when the concentration is higher the morphology changes, this could be because of the placement of the nanoparticles in the PS domains, what provokes a decrease on the mobility of the domains[46]. This fact could cause the morphology not to evolve enough to reach the same morphology as the neat block copolymer. However, a very good dispersion of nanoparticles is obtained for all nanocomposites, showing the efficiency of nanoparticle modification for increasing the compatibility with the matrix.

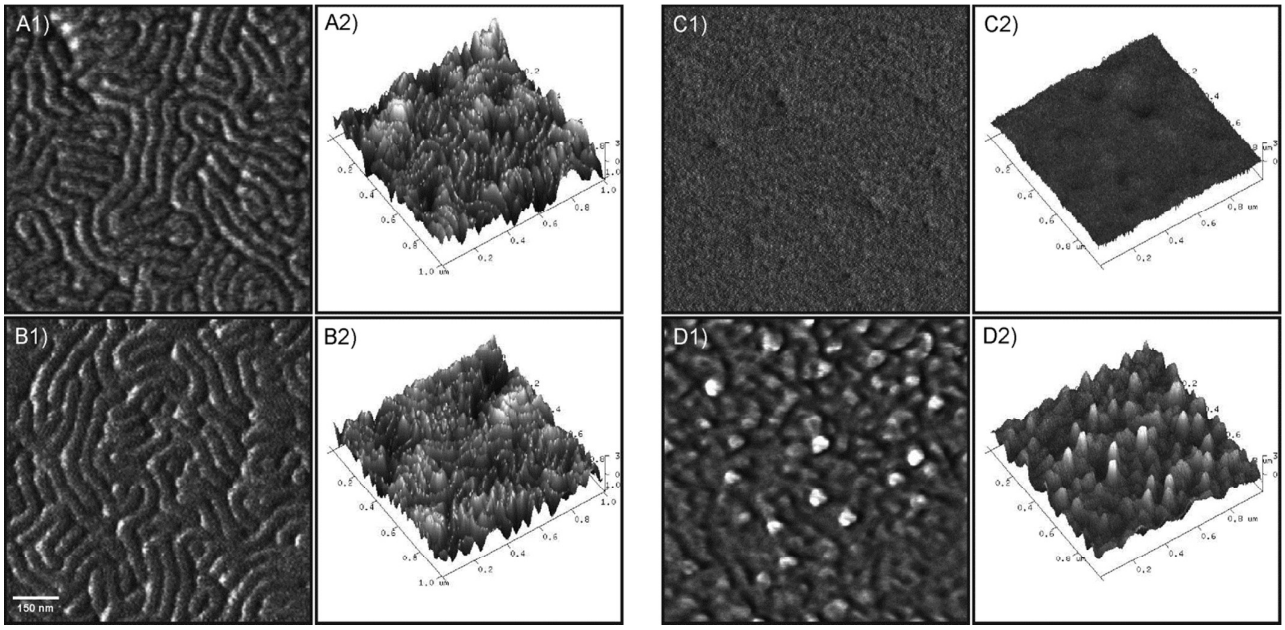

Figure 5. AFM phase (1) and 3D height (2) images of A) neat block copolymer, B) nanocomposite with 1 wt% of nanoparticles after 48 h of exposure to dioxane, and AFM phase (1) and 3D height (2) images of C) neat block copolymer and D) nanocomposite with 1 wt% of nanoparticles after 6 hours of exposure to UV light irradiation

UV light irradiation degradation

As nanoparticles cannot be seen by AFM, their presence and placement at the PS domains of the diblock copolymer can be corroborated by removing the organic part of the nanocomposites by exposure to UV light irradiation[47]. Figure 5 shows the AFM images of the neat block copolymer and nanocomposites with 1 wt% of nanoparticles before and after exposure to UV light irradiation for 6 h. While the copolymer is removed by UV radiation (see Figures 5A and 5C), by comparing Figures 5B and 5D it can be seen that the nanoparticles are located mainly at the PS domain of the block copolymer, detected by AFM as bright points rising from the partially degraded PS domains.

Magnetic properties measurements

Figure 6 shows the magnetic characterization results of the nanocomposites with 5 wt% of nanoparticles as an example (similar results were obtained for the rest of nanocomposites prepared). The inorganic/organic nanocomposites exhibit a typical superparamagnetic behavior at room temperature and ferromagnetic one at low temperatures[47, 48]. Below the blocking temperature (T_b) (~250 K) the field-cooled (FC) and zero-field-cooled (ZFC) magnetization curves diverge, magnetic moment are singledomain, pinned by anisotropy at low temperature and thermally disordered above the blocking temperature. Apart from FC/ZFC curves the hysteresis loops were also measured at different temperatures of 2, 100 and 300 K (Figure 6B). Below the blocking temperature the hysteresis loops are hysteretic and non-hysteretic above the T_b, with the appreciation of smooth hysteresis at 100 K. At the magnetization curve M *vs* B at 2 K the hysteresis is observed with a coercivity of approximately 175 Oe and a remanence of $5.6 \cdot 10^{-5}$ emu, whereas above the blocking temperature both the coercivity and remanence are zero, demonstrating the superparamagnetic behavior of the final nanocomposites[49, 50].

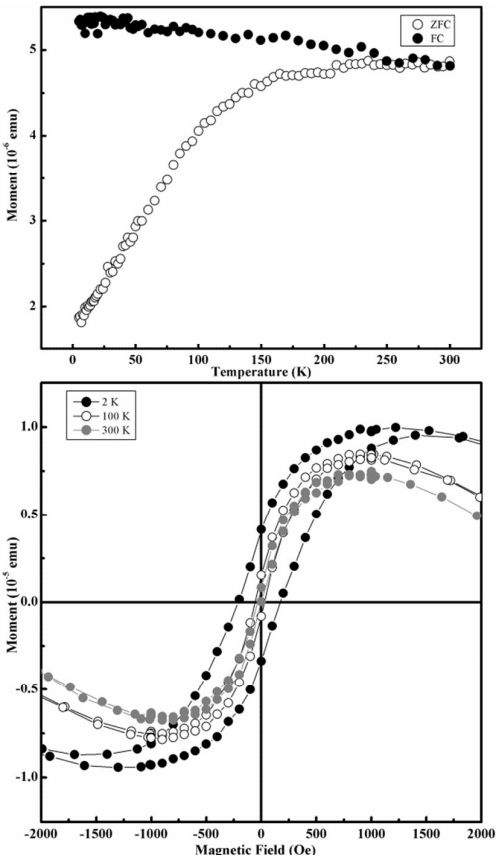

Figure 6. Magnetic properties of nanocomposites with 5 wt% of nanoparticles, A) ZFC and FC curves at 100 Oe and B) M *vs* H curves at 2, 100 and 300 K (B include diamagnetic contribution from the block copolymer matrix and sample holder. These contributions are sufficient to produce a negative slope at high fields)

Conclusions

In this work maghemite nanoparticles were modified successfully by *grafting through* technique, as it was corroborated by FTIR and TGA. This functionalization of the nanoparticle with PS polymer brushes was adequate to disperse the iron oxide nanoparticles through the PS-*b*-P4VP block copolymer. Very good dispersions, without any remarkable agglomerates, were obtained. The addition of the nanoparticles affected the nanostructuring of the block copolymer. When neat block copolymer was exposed to dioxane vapors for 24 h, a hexagonal morphology was obtained, changing to a stripped one for longer exposure time of 48 h. But as the addition of the nanoparticles seemed to reduce the mobility of the PS domain, the formation of a totally stripped morphology after 48 h of exposure was not obtained. This fact seemed to indicate the presence of nanoparticles at PS domains as confirmed after removing the organic part of nanocomposites by UV radiation. Moreover, the successful transference of magnetic properties of nanoparticles to the nanocomposites was demonstrated by measuring magnetic properties.

Acknowledgements

Financial support from the Basque Country Government (Grupos Consolidados, IT-365-07) and the Ministry of Economy and Competitiveness (MAT 2012-31675) is gratefully acknowledged. The technical and human support provided by SGIker (Magnetic Measurements) of UPV/EHU. I.B. thanks Euskal Herriko Unibertsitatea/Universidad del País Vasco for Ph.D Fellowship (Becas de Formación de Investigadores 2011 (PIF/UPV/11/030)).

References

1 M.R. Bockstaller, R.A. Mickiewicz and E.L. Thomas, *Adv. Mater.,* 2005, **17,** 1331.
2 M. Lazzari and M.A. López-Quintela, *Adv. Mater.,* 2003, **15**, 1583.
3 T.N. Hoheisel, K. Hur and U.B. Wiesner, *Progress in Polymer Science*, 2015, **40**, 3.
4 L. Peponi, A. Tercjak, J. Gutierrez, H. Stadler, L. Torre, J.M. Kenny and I. Mondragon, *Macromol Matert Eng*, 2008, **293**, 568.
5 J. Gutierrez, A. Tercjak, L. Peponi and I. Mondragon, *J. Phys. Chem. C,* 2009, **113**, 8601.
6 H. Etxeberria, A. Tercjak, I. Mondragon, A. Eceiza and G. Kortaberria, *Collod Polym Sci,* 2014, **292**, 229.
7 Garcia, A. Tercjak, J. Gutierrez, L. Rueda and I. Mondragon, *J. Phys. Chem. C,* 2008, **112**, 14343.
8 Y. Yao, E. Metwalli, B. Su, V. Körstgens, D. Moseguí González, A. Miasnikova, A. Laschewsky, M. Opel, G. Santoro, S.V. Roth and P. Müller-Buschbaum, *Appl. Mater. Interfaces*, 2015, **7**, 13080.
9 S. Park, D.H. Lee, J. Xu, B. Kim, S.W. Hong, U. Jeong, T. Xu and T.P. Russell, *Science*, 2009, **323**, 1030.
10 Y.H. Jang, X. Xin, M. Byun, Y.J. Jang, Z. Lin and D.H. Kim, *Nano Lett.* 2012, **12**, 479.
11 S.B. Darling, N.A. Yufa, A.L. Cisse, S.D. Bader and S.J. Sibener, *Adv. Mater.* 2005, **17**, 2446
12 C. Xu, K. Ohno, V. Ladmiral and R.J. Composto, *Polymer* 2008, **49**, 3568.
13 J. Wu, H. Li, S. Wu, G. Huang, W. Xing, M. Tang and Q. Fu, *J. Phys. Chem. B* 2014, **118**, 2186.
14 W. Lu, Y. Shen, A. Xie and W. Zhang, *Journal of Magnetism and Magnetic Materials* 2013, **345**, 142.
15 A. Horechyy, B. Nandan, N.E. Zafeiropoulos, P. Formanek, U. Oertel, N.C. Bigall, A. Eychmüller And M. Stamm, *Adv. Funct. Mater*. 2013, **23**, 483.
16 C.-T. Lo, Y.-C. Chang, S-C. Wu and C.-L. Lee, *Colloids and Surfaces A: Physicochem. Eng. Aspects* 2010, **368**, 6.
17 M.J. Fasolka and A.M. Mayes, *Annu Rev Mater Res* 2001, **31**, 323.
18 F.S. Bates and G.H. Fredickson, *Annu Rev Phys Chem* 1990, **41**, 525.
19 R.J. Albalak, E.L. Thomas and M.S. Capel, *Polymer* 1997, **38**, 3819.
20 T. Xu, H.C. Kim, J. DeRouchey, C. Seney, C. Levesque, P. Martin, C.M. Stafford and T.P. Russell, *Polymer* 2001, **42**, 9091.
21 W.H. Huang, P.Y. Chen and S.H. Tung, *Macromolecules* 2012, **45**, 1562.
22 T.L. Morkved, M. Lu, A.M. Urbas, E.E. Ehrichs, H.M. Jaeger, P. Mansky and T.P. Russell, *Science* 1996, **273**, 931.
23 T. Thurn-Albrecht, J. DeRouched and T.P. Russell, *Macromolecules* 2002, **3**, 3250.
24 M.P. Stoykovich, M. Müller, S.O. Kim, H.H. Solak, E.W. Edwards, J.J. de Pablo and P.F. Nealey, *Science* 2005, **308**, 1442.
25 R.A. Segalman, A. Hexemer and E.J. Kramer, *Physical Review Letter* 2003, **91**, 196101.
26 C. De Rosa, C. Park, E.L. Thomas and B. Lotz, *Nature* 2004, **405**, 433.
27 D.W. Van Krevelen, Properties of Polymers, Elsevier Scientific Publishing Sons,1989, New York
28 S. Zou, R. Hong, T. Emrick and G.C. Walker, *Langmuir* 2007, **23**, 1612.
29 Q. Zhang, T. Xu, D. Butterfield, M.J. Misner, D.Y. Ryu, T. Emrick and T.P. Russel, *Nano Lett* 2005, **5**, 357.
30 Y. Boontongkong and R.E. Cohen, *Macromolecules* 2002, **35**, 3647.
31 G. Mountrichas, S. Pispas and N. Tagmatarchis, *Mater Sci Eng B* 2008, **152**, 40.
32 I. Barandiaran, A. Cappelletti, M. Strumia, A. Eceiza and G. Kortaberria, *Eur Polym J* 2014, **58**, 226.
33 S.J. Park, M.S. Cho, S.T. Lim, H.J. Choi and M.S. Jhon, *Macromol Rapid Commun* 2003, **24**, 1070.
34 G. Xu, W.T. Wu, Y. Wang, W. Pang, Q. Zhu, P. Wang and Y. You, *Polymer* 2006, **47**, 5909.
35 M. Kim, C.K. Hong, S. Choe and S.E. Shim, *J Polym Sci Part A: Polym Chem* 2007, **45**, 4413.
36 M. Henze, D. Madge, O. Prucker and J. Ruhe, *Macromolecules* 2014, **47**, 2929.
37 I. Barandiaran and G. Kortaberria, *Eur Polym J* 2015, **68**, 57.
38 B. Radhakrishnan, R. Ranjan and W.J. Brittain, *Soft Matter* 2006, **2**, 386.
39 H. Etxeberria, I. Zalakain, M. Mondragon, A. Eceiza and G. Kortaberria, *Colloid Polym Sci* 2013, **291**, 1881.
40 Y. Sun, X. Ding, Z. Zheng, X. Cheng, X. Hu and Y. Peng, *Eur Polym J* 2007, **43**, 762.
41 H. Etxeberria, I. Zalakain, R. Fernandez and G. Kortaberria, *Colloid Polym Sci* 2013, **291**, 633.
42 R. Mueller, H.K. Kammler, K. Wegner and S.E. Pratsinis, *Langmuir* 2003, **19**, 160.
43 M.A. Rodriguez, M.J. Liso, F. Rubio, J. Rubio and J.L. Oteo, *Journal of Materials Science* 1999, **34**, 3867.
44 C. Bartholome, E. Beyou, E. Bourgeat-Lami, P. Chaumont and N. Zydowicz, *Macromolecules* 2003, **36**, 7946.

45 R. Fernandez, H. Etxeberria, A. Eceiza and A. Tercjak, *Eur. Polym. J.* 2013 **49**, 984.
46 H. Etxeberria, R. Fernandez, I. Zalakain, I. Mondragon, A. Eceiza and G. Kortaberria, *Journal of Colloid and Interface Science* 2014, **416**, 25.
47 J. Gutierrez, A. Tercjak, I. Garcia and I. Mondragon, *Nanotechnology* 2009, 20, 225603 (9pp).
48 H. Zeng, C.T. Black, R.L. Sandstrom, P.M. Rice, C.B. Murray and S. Sun, *Physical Reviw B* 2006, **73**, 020402(R).
49 C.P. Bean and J.D. Livingston, *J. Appl. Phys.* 1959, **30**, S120.
50 L. Schulz, W. Schirmacher, A. Omran, V.R. Shah, P. Böni, W. Petry and P. Müller-Buschbaum, *J. Phys.: Condens. Matter* 2010, **22**, 346008 (6pp).
51 C. Xu, K. Ohno, V. Ladmiral, D.E. Milkie, J.M. Kikkawa and R.J. Composto, R.J. *Macromolecules* 2009, **42**, 1219.

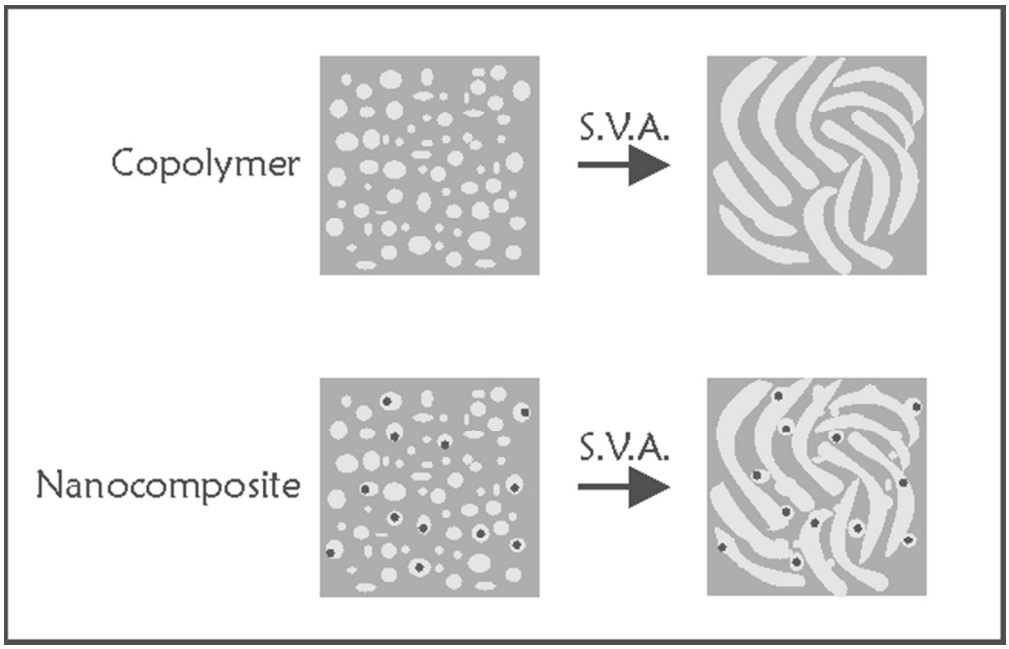

55x35mm (300 x 300 DPI)